

Text-to-Image Diffusion Models are Zero-Shot Classifiers

Kevin Clark ^{*1} Priyank Jaini ^{*1}

Abstract

The excellent generative capabilities of text-to-image diffusion models suggest they learn informative representations of image-text data. However, what knowledge their representations capture is not fully understood, and they have not been thoroughly explored on downstream tasks. We investigate diffusion models by proposing a method for evaluating them as zero-shot classifiers. The key idea is using a diffusion model’s ability to denoise a noised image given a text description of a label as a proxy for that label’s likelihood. We apply our method to Imagen, using it to probe fine-grained aspects of Imagen’s knowledge and comparing it with CLIP’s zero-shot abilities. Imagen performs competitively with CLIP on a wide range of zero-shot image classification datasets. Additionally, it achieves state-of-the-art results on shape/texture bias tests and can successfully perform attribute binding while CLIP cannot. Although generative pre-training is prevalent in NLP, visual foundation models often use other methods such as contrastive learning. Based on our findings, we argue that generative pre-training should be explored as a compelling alternative for vision and vision-language problems.

1. Introduction

Large models pre-trained on internet-scale data can adapt effectively to a variety of downstream tasks. Increasingly, they are being used as zero-shot learners with no task-specific training, such as with CLIP (Radford et al., 2021) for images and GPT-3 (Brown et al., 2020) for text. In natural language processing, many successful pre-trained models are generative (i.e., language models). However, generative pre-training is less commonly used for visual tasks. Until recently, the usual practice for vision problems was to pre-train models on labeled datasets such as Imagenet (Deng

^{*}Equal contribution ¹Google Research, Brain Team, Toronto, Ontario, Canada.. Correspondence to: Kevin Clark <kevclark@google.com>, Priyank Jaini <pjaini@google.com>.

et al., 2009), or JFT (Sun et al., 2017). Later research in visual and vision-language problems has led to image-text models pre-trained primarily using either contrastive losses (Radford et al., 2021; Jia et al., 2021; Yuan et al., 2021) or autoencoding tasks (Vincent et al., 2010; He et al., 2022).

On the other hand, generative text-to-image models based on denoising diffusion probabilistic models (Ho et al., 2020) such as Imagen (Saharia et al., 2022a), Dalle-2 (Ramesh et al., 2022), and Stable Diffusion (Rombach et al., 2022) can generate realistic high-resolution images and generalize to diverse text prompts. Their strong performance suggests that they learn effective representations of image-text data. However, their ability to transfer to downstream discriminative tasks and how they compare to other pre-trained models has not been explored thoroughly.

In this paper, we investigate these questions by transferring the Imagen diffusion model to discriminative tasks. Specifically, we propose a method for using text-to-image diffusion models as zero-shot image classifiers. While Burgert et al. (2022) explore using Stable Diffusion for zero-shot referring segmentation and Bar et al. (2022) use inpainting models for few-shot pixel-level tasks like edge detection and style transfer, to our knowledge zero-shot classification with diffusion models has not been studied previously.

Our method essentially runs Imagen as a generative classifier (Ng & Jordan, 2001), using a re-weighted version of Imagen’s variational lower bound to score images since diffusion models do not produce exact likelihoods. First, our method makes a text prompt for each class (e.g. “a photo of a cat.”). Then it scores the input image conditioned on each text prompt, measuring how helpful each prompt is for denoising the image averaged over different noise levels. The class corresponding to the prompt with the best score is predicted. This classification procedure requires denoising with Imagen many times for every class (with different noise levels), so it is computationally expensive. To make it usable in practice, we present improvements that increase the method’s sample efficiency by up to 1000x, such as pruning obviously-incorrect classes early. While still requiring too much compute to be an easily-deployable classifier, our methodology allows us to quantitatively study fine-grained aspects of a diffusion model’s learned knowledge through evaluation on classification tasks (as opposed

to qualitatively examining model generations).

We compare Imagen against CLIP¹ (Radford et al., 2021), a widely used model for zero-shot image-text tasks trained with contrastive learning. A high-level goal of the experiments is to see the strengths and weaknesses of generative and contrastive pre-training for computer vision. First, we demonstrate that Imagen has strong zero-shot classification accuracies (competitive with CLIP) on several diverse vision datasets. Next, we show Imagen performs remarkably well on Stylized ImageNet (Geirhos et al., 2019), where images have been stylized with textures conflicting with their labels. Imagen achieves >50% error reduction over CLIP and even outperforms the much larger ViT-22B (Dehghani et al., 2023) model. This finding is particularly interesting because, unlike supervised classifiers, humans are known to be much more reliant on shape than texture when identifying images. We also show that it is possible to obtain fairly well-calibrated confidence scores from our classifier, despite it not producing precise probabilities for classes. Lastly, we study attribute binding in Imagen using the synthetic data from Lewis et al. (2022), and find that, unlike CLIP, it can successfully bind together attributes in some settings.

The main contributions of this paper are:

- We show text-to-image diffusion models can be used as effective zero-shot classifiers. While using too much compute to be very practical on downstream tasks, the method provides a way of quantitatively studying what the models learn.
- We develop techniques that hugely lower the compute cost of these zero-shot classifiers, making them usable (although still slow) on datasets with many classes.
- We demonstrate the strong generalization capabilities of Imagen, resulting in good zero-shot performance on vision datasets (comparable to CLIP). We further show these classifiers can produce calibrated scores.
- We show Imagen is robust to misleading textural cues, achieving excellent results on Stylized Imagenet.
- We use our framework to study attribute binding in Imagen and find that it can perform some binding tasks while CLIP generally cannot.

Together, our study of Imagen suggests that text-to-image diffusion models learn powerful representations that can effectively be transferred to tasks beyond image generation.

2. Preliminaries

We begin by recalling background knowledge on diffusion models (Sohl-Dickstein et al., 2015; Ho et al., 2020; Song

¹We use ViT-L/14, the largest public CLIP model

et al., 2020; Song & Ermon, 2020) and recent advances on text-to-image diffusion models.

Diffusion Models: Diffusion models are latent variable generative models defined by a forward and reverse Markov chain. Given an unknown data distribution, $q(\mathbf{x}_0)$, over observations, $\mathbf{x}_0 \in \mathbb{R}^d$, the forward process corrupts the data into a sequence of noisy latent variables, $\mathbf{x}_{1:T} := \{\mathbf{x}_1, \mathbf{x}_2, \dots, \mathbf{x}_T\}$, by gradually adding Gaussian noise with a fixed schedule defined as:

$$q(\mathbf{x}_{1:T} | \mathbf{x}_0) := \prod_{t=1}^T q(\mathbf{x}_t | \mathbf{x}_{t-1}) \quad (1)$$

where $q(\mathbf{x}_t | \mathbf{x}_{t-1}) := \text{Normal}(\mathbf{x}_t; \sqrt{1 - \beta_t} \mathbf{x}_{t-1}, \beta_t \mathbf{I})$.

The reverse Markov process gradually denoises the latent variables to the data distribution with learned Gaussian transitions starting from $\text{Normal}(\mathbf{x}_T; 0, \mathbf{I})$ i.e.

$$p_{\theta}(\mathbf{x}_{0:T}) := p(\mathbf{x}_T) \cdot \prod_{t=0}^{T-1} p_{\theta}(\mathbf{x}_{t-1} | \mathbf{x}_t)$$

$p_{\theta}(\mathbf{x}_{t-1} | \mathbf{x}_t) := \text{Normal}(\mathbf{x}_{t-1}; \mu_{\theta}(\mathbf{x}_t, t), \Sigma_{\theta}(\mathbf{x}_t, t))$. The aim of the denoising process is for the forward process distribution $\{\mathbf{x}_t\}_{t=0}^T$ to match that of the reverse process $\{\tilde{\mathbf{x}}_t\}_{t=0}^T$ i.e., the generative model $p_{\theta}(\mathbf{x}_0)$ closely matches the data distribution $q(\mathbf{x}_0)$. Specifically, these models can be trained by optimizing the variational lower bound of the marginal likelihood (Kingma et al., 2021; Ho et al., 2020):

$$-\log p_{\theta}(\mathbf{x}_0) \leq -\text{VLB}(\mathbf{x}_0) := \mathcal{L}_{\text{Prior}} + \mathcal{L}_{\text{Recon}} + \mathcal{L}_{\text{Diffusion}}$$

$\mathcal{L}_{\text{Prior}}$ and $\mathcal{L}_{\text{Recon}}$ are the prior and reconstruction loss that can be estimated using standard techniques in the literature (Kingma & Welling, 2014). The diffusion loss, $\mathcal{L}_{\text{Diffusion}}$, is:

$$\mathcal{L}_{\text{Diffusion}} := \sum_{t=1}^T \mathbb{E}_{q(\mathbf{x}_t | \mathbf{x}_0)} \mathbb{D}_{\text{KL}} \left[q(\mathbf{x}_{t-1} | \mathbf{x}_t, \mathbf{x}_0) || p_{\theta}(\mathbf{x}_{t-1} | \mathbf{x}_t) \right]$$

Following Kingma et al. (2021), the (re-weighted) diffusion loss can be written in simplified form as:

$$\mathcal{L}_{\text{Diffusion}} = \mathbb{E}_{\mathbf{x}_0, \mathbf{\epsilon}, t} \left[\mathbf{w}_t \|\mathbf{x}_0 - \tilde{\mathbf{x}}_{\theta}(\mathbf{x}_t, t)\|_2^2 \right]$$

with $\mathbf{x}_0 \sim q(\mathbf{x}_0)$, $\mathbf{\epsilon} \sim \text{Normal}(0, \mathbf{I})$, and $t \sim \mathcal{U}([0, T])$. Here, \mathbf{w}_t is a weight assigned to the timestep, and $\tilde{\mathbf{x}}_{\theta}(\mathbf{x}_t, t)$ is the model's prediction of the observation \mathbf{x}_0 from the noised observation \mathbf{x}_t .

Diffusion models can be conditioned on additional inputs like class labels, text prompts, segmentation masks or low-resolution images. A conditional diffusion model is trained using the following modified diffusion loss from Equation (2):

$$\mathcal{L}_{\text{Diffusion}} = \mathbb{E}_{(\mathbf{x}_0, \mathbf{y}), \mathbf{\epsilon}, t} \left[\mathbf{w}_t \|\mathbf{x}_0 - \tilde{\mathbf{x}}_{\theta}(\mathbf{x}_t, \mathbf{y}, t)\|_2^2 \right] \quad (2)$$

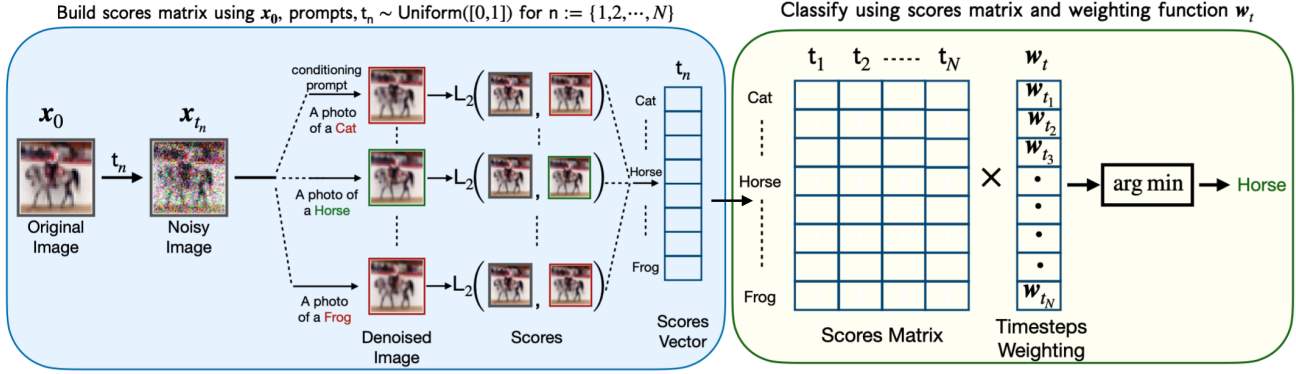


Figure 1. Zero-Shot Classification using Imagen. We first calculate scores for each label prompt across multiple time-steps to generate a scores matrix. We then classify an image by aggregating the scores for each class using a weighting function over the time-steps. The image is assigned the class with the minimum aggregate score. In Section 3.1, we discuss how efficiency can be improved only computing a subset of the full scores matrix.

where y is the conditioning input for each data point. In this paper we use Imagen, a text-conditioned diffusion model that comprises of a frozen T5 (Raffel et al., 2020) language encoder that encodes an input prompt into a sequence of embeddings, a 64×64 image diffusion model, and two cascaded super-resolution diffusion models that generate 256×256 and 1024×1024 images.

3. Zero-Shot Classification using Imagen

In this section, we show how to convert the generation process of a text-to-image diffusion model into a zero-shot classifier to facilitate quantitative evaluation on downstream tasks. Figure 1 shows an overview of our method.

Imagen as a Generative Classifier: We begin with a dataset, $\{(\mathbf{x}^1, y^1), \dots, (\mathbf{x}^n, y^n)\} \subseteq \mathbb{R}^{d_1 \times d_2} \times [y_K]$ of n images² where each image belongs to one of K classes $[y_K] := \{y_1, y_2, \dots, y_K\}$. Given an image \mathbf{x} , our goal is to predict the most probable class assignment

$$\begin{aligned}\tilde{y} &= \arg \max_{y_k} p(y = y_k | \mathbf{x}) \\ &= \arg \max_{y_k} p(\mathbf{x} | y = y_k) \cdot p(y = y_k) \\ &= \arg \max_{y_k} \log p(\mathbf{x} | y = y_k).\end{aligned}$$

where we assume a uniform prior $p(y_i = y_k) = \frac{1}{k}$ that can be dropped from the $\arg \max$.³ A generative classifier (Ng & Jordan, 2001) uses a conditional generative model with parameters θ to estimate the likelihood as $p_\theta(\mathbf{x} | y = y_k)$.

Using Imagen as a generative classifier requires two modifications. First, Imagen is conditioned on text prompts

rather than class labels. Thus we convert each label, y_k , to text using a mapping ϕ with a dataset-specific template (e.g. $y_k \rightarrow$ A photo of a y_k). Second, diffusion models do not produce exact log-likelihoods (i.e. we cannot compute $\log p_\theta(\mathbf{x} | y = y_k)$ directly). Our key idea for a solution is to use the VLB (more specifically $\mathcal{L}_{\text{Diffusion}}$ as Imagen is not trained with the other losses) as a proxy. Thus we have:

$$\begin{aligned}\tilde{y} &= \arg \max_{y_k} \log p_\theta(\mathbf{x} | y = y_k) \\ &\approx \arg \min_{y_k} \mathcal{L}_{\text{Diffusion}}(\mathbf{x}, y_k) \\ &= \arg \min_{y_k \in [y_K]} \mathbb{E}_{\epsilon, t} \left[\mathbf{w}_t \|\mathbf{x} - \tilde{\mathbf{x}}_\theta(\mathbf{x}_t, \phi(y_k), t)\|_2^2 \right]\end{aligned}\quad (3)$$

Estimating the Expectation: We approximate the expectation in Equation (3) using Monte-Carlo estimation. At each step, we sample a $t \sim \mathcal{U}([0, 1])$ and then a \mathbf{x}_t according to the forward diffusion process (Equation (1)): $\mathbf{x}_t \sim q(\mathbf{x}_t | \mathbf{x}_0)$. Next, we denoise this noisy image using Imagen (i.e. we use Imagen to predict \mathbf{x} from \mathbf{x}_t), obtaining $\hat{\mathbf{x}} = \tilde{\mathbf{x}}_\theta(\mathbf{x}_t, \phi(y_k), t)$. We call the squared error of the prediction, $\|\mathbf{x} - \hat{\mathbf{x}}\|_2^2$, a *score* for (\mathbf{x}, y_k) . We score each class N times, obtaining a $K \times N$ *scores matrix*⁴ for the image. Finally, we weight the scores according to the corresponding \mathbf{w}_t and take the mean, resulting in an estimate of $\mathcal{L}_{\text{Diffusion}}$ for each class.

Prompt Ensembling: Similar to the zero-shot classification setting for CLIP in Radford et al. (2021), we could also consider an ensemble of prompts in Equation (3) for classification instead of using a single prompt template (i.e. the expectation is also over different prompt templates). While this would boost classification accuracy, we generally use

²For simplicity, we use \mathbf{x} in place of \mathbf{x}_0 to refer to an image.

³We can't use a learned prior in the zero-shot setting.

⁴Later we discuss how we can avoid computing the full matrix for efficiency.

only a single prompt for the sake of simplicity and efficiency, as our goal is to better understand models rather than achieve state-of-the-art zero-shot performance.

Choice of Weighting Function: The choice of weighting function, w_t , in Equation (3) is critical to the overall performance of the classification algorithm. One option is learning an effective weighting function w_t . We do this by binning the times into 20 buckets and training a 20-features logistic regression model that learns weights for those buckets that maximize classification accuracy. However, using such a learned weighting is not truly zero-shot since it requires label information to learn.

We thus also handcrafted a weighting function that can be used across datasets. We designed w_t by finding a simple function that looked close to our learned weighting function on CIFAR-100. In particular, we found that $w_t := \exp(-7t)$ works well across many datasets and used it for our experiments. As it is monotonic, $\mathcal{L}_{\text{Diffusion}}$ with this weighting can still be viewed as a likelihood-based objective that maximizes the variational lower bound under simple data augmentations (Kingma & Gao, 2023).

3.1. Improving Efficiency

Computing \tilde{y} with naive Monte-Carlo estimation can be expensive because $\mathcal{L}_{\text{Diffusion}}$ has fairly high variance. Here, we propose techniques that reduce the compute cost of estimating the arg min over classes. The key idea is to leverage the fact that we only need to compute the arg min and do not require good estimates of the actual expectations.

Shared Noise: Differences between individual Monte-Carlo samples from $\mathcal{L}_{\text{Diffusion}}$ can of course be due to different t or forward diffusion samples from $q(\mathbf{x}_t | \mathbf{x}_{t-1})$, whereas we are only interested in the effect of the text conditioning $\phi(y_k)$. We find far fewer samples are necessary when we use the *same* t and \mathbf{x}_t across different classes, as shown in Figure 1. In other words, after sampling a $t \sim \mathcal{U}([0, 1])$ and $\mathbf{x}_t \sim q(\mathbf{x}_t | \mathbf{x}_0)$, we score all classes against this noised image instead of a single one. As a result, the differences between these estimates are only due to the different text conditioning signals.

Candidate Class Pruning: Rather than using the same amount of compute to estimate the expectation for each class, we can further improve efficiency by discarding implausible classes early and dynamically allocating more compute to plausible ones. In particular, we maintain a set of candidate classes for the image being classified. After collecting a new set of scores for each candidate class, we discard classes that are unlikely to become the lowest-scoring (i.e. predicted) class with more samples. Since we are collecting paired samples (with the same t and $\hat{\mathbf{x}}_{i,t}$), we

Algorithm 1 Diffusion model classification with pruning.

given: Example to classify \mathbf{x} , diffusion model w/ params θ , weighting function w , hyperparameters `min_scores`, `max_scores`, `cutoff_pval`.

//Map from classes to weighted diffusion model scores.
 $\text{scores} = \{y_i : [] \text{ for } y_i \in [y_K]\}$
 $n = 0$
while $|\text{scores}| > 1$ **and** $n < \text{max_scores}$:
 $n = n + 1$
//Noise the image
 $t \sim \mathcal{U}([0, 1])$
 $\mathbf{x}_t \sim q(\mathbf{x}_t | \mathbf{x})$
//Score against the remaining classes.
for $y_i \in \text{scores}$:
 add $w_t \|\mathbf{x} - \tilde{\mathbf{x}}_\theta(\mathbf{x}_t, \phi(y_i), t)\|_2^2$ to $\text{scores}[y_i]$
//Prune away implausible classes.
 $\tilde{y} = \arg \min_{y_i} \text{scores}[y_i].\text{mean}()$
if $n \geq \text{min_scores}$:
 for $y_i \in \text{scores}$:
 if paired_ttest_pval(
 $\text{scores}[\tilde{y}], \text{scores}[y_i]) < \text{cutoff_pval}$:
 remove y_i from scores .
return \tilde{y}

use a paired student's t-test to identify classes that can be pruned. Our scores, of course, do not exactly follow the standard assumptions of a student's t-test (e.g. they are not normally distributed), so we use a small p-value ($2e^{-3}$ in our experiments) and ensure each class is scored a minimum number of times (20 in our experiments) to minimize the chance of pruning the correct class. The full procedure is shown in Algorithm 1.

Comparison: Figure 2 compares the number of samples needed to accurately classify CIFAR-100 images for different methods. Using shared noise and pruning greatly improves efficiency, requiring up to 1000x less compute than naïve scoring. Nevertheless, classifying with a diffusion model still typically takes 10s of scores per class on average, making the diffusion classifier expensive to use for datasets with many classes.

4. Empirical Analysis and Results

In this section, we detail our analysis for the zero-shot classifier based on Imagen for a variety of tasks. These include classification on various vision datasets to study generalization capabilities on diverse domains, evaluating of the model's robustness to conflicting cues between texture and shape, and studying attribute binding ability through targeted evaluation on synthetic data.

We compare Imagen with CLIP (Radford et al., 2021),

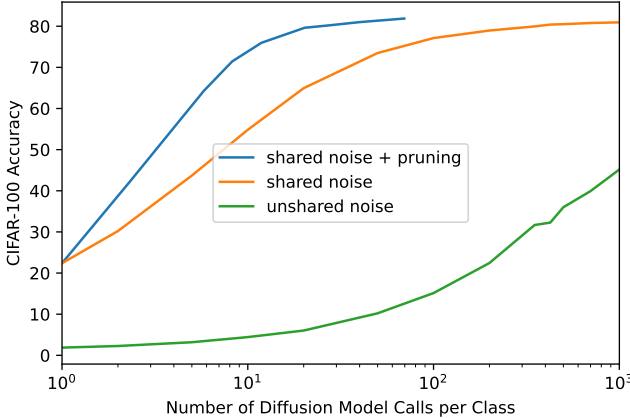


Figure 2. Comparison of efficiency improvements on CIFAR-100. Shared noise improves sample efficiency by roughly 100x and pruning by an additional 8-10x.

which is widely used as a zero-shot classifier. Our main aim is to study the strengths and weaknesses of image-text representation learning via generative training as in Imagen and contrastive training as used for CLIP.

Imagen details: We use the 2B parameter Imagen model for 64×64 resolution text-to-image synthesis. It is trained using a batch size of 2048 for 2.5M training steps on a combination of internal datasets, with around 460M image-text pairs, and the publicly available Laion dataset (Schuhmann et al., 2021), with 400M image-text pairs. We only use the 64×64 model in our experiments because we found the high-resolution models to work less effectively as classifiers. The high-resolution models condition strongly on their low-resolution inputs and are therefore less sensitive to the text prompt.

CLIP details: CLIP encodes image features using a ViT-like transformer (Dosovitskiy et al., 2021) and uses a causal language model to get the text features. After encoding the image and text features to a latent space with identical dimensions, it evaluates a similarity score between these features. CLIP is pre-trained using contrastive learning. Here, we compare to the largest CLIP model (with a ViT-L/14@224px as the image encoder). The model is smaller than Imagen (400M parameters), but is trained for longer (12.8B images processed vs 5.B). While Imagen was trained primarily as a generative model, CLIP was primarily engineered to be transferred effectively to downstream tasks.

Experiment details: For each experiment, we obtain scores using the efficient scoring method in Algorithm 1. Nevertheless, due to the still-substantial compute cost, we use reduced-size datasets (4096 examples) for our experiments. We preprocess each dataset by normalizing the images, performing a central crop and then resizing the

images to 64×64 resolution. We use $\text{min_scores} = 20$, $\text{max_scores} = 2000$, and $\text{cutoff_pval} = 2 \times e^{-3}$. Since we use a fixed single prompt template to obtain results for Imagen, we follow the same setting for CLIP to keep the results comparable. Therefore, our reported results are often lower than in the CLIP paper, which uses prompt ensembling.

Comparing models: Imagen and CLIP have different model sizes and are trained on different datasets for different amounts of time, so the comparison is not direct. While ideally we would train models of the same size on the same data, this would be very expensive and challenging in practice; we instead used two strong existing pre-trained models. Our comparisons are geared towards highlighting the strengths and weaknesses of Imagen.

4.1. Image Classification

Setup: We first evaluate the performance of Imagen at zero-shot classification. For this purpose, we consider 13 datasets from Radford et al. (2021) as reported in Table 1. We report the best accuracy achieved by Imagen using two weighting functions, w_t : (a) *hand-engineered* weights across noise levels, $w_t := \exp(-7t)$ and, (b) learned weights.

We use the prompt templates and class labels used by Radford et al. (2021), which renames some classes that confuse models (e.g. “crane → “crane bird”” in Imagenet) (OpenAI, 2021b). We use the first prompt from the list, except for Imagenet, where we use “A bad photo of a *label*” since this is a good prompt for both Imagen and CLIP (OpenAI, 2021a). We found in our experiments that our model was quite robust to the choice of prompt. For example, we tried four different prompts from the CLIP templates for CIFAR-100 and found accuracies to all be within 1.5% of each other.

Since we use the low-resolution Imagen model, we obtain results using CLIP under two settings for a fair comparison. In the first setting, we resize all the datasets to 64×64 which serves as the base low-resolution dataset. Imagen uses this dataset directly. For CLIP, we subsequently upsample the images and resize them to 224×224 resolution, followed by a central crop and normalization as used in Radford et al. (2021). In the second setting, we directly resize all datasets to 224×224 resolution, followed by a central crop and normalization to obtain the best results possible using CLIP where it can take advantage of its higher input resolution.

Results: Results are shown in Table 1. The first eight datasets (up through EuroSAT) are all originally of resolution 64×64 or less. On all these datasets, Imagen outperforms CLIP on classification accuracy under the same evaluation setting i.e. the models are conditioned on the same text prompts, etc. Imagen significantly outperforms

Dataset	Imagen	CLIP
CIFAR10	96.6	94.7
CIFAR100	84.3	68.6
STL10	99.6	99.6
MNIST	79.2	74.3
DTD	37.3	36.0
Patch Camelyon	60.3	58.0
SVHN	62.7	21.50
EuroSAT	60.3	58.04
Stanford Cars	81.0	62.8 / 75.8
Imagenet	62.7	63.4 / 75.1
Caltech101	68.9	70.2 / 84.1
Oxford Pets	66.5	76.0 / 89.9
Food 101	68.4	83.9 / 93.3

Table 1. Percent accuracies for zero-shot image classification. For CLIP where two numbers are reported, the accuracy correspond to two settings: downsizing the images to 64x64 and then resizing the images up to 224x224 (so CLIP does not have an advantage in input resolution over the 64x64 Imagen model) and resizing the images directly to 224x224 (so CLIP has the advantage of higher resolution). The top 8 datasets have a resolution of 64x64 or less. Variances in accuracy are <1% across different random seeds.

CLIP on e.g. SVHN, which requires recognizing text in an image. Saharia et al. (2022b) observe that Imagen is particularly good at generating text, so this finding suggests Imagen’s areas of strength in generation carry over to downstream tasks.

The next five datasets use higher-resolution images. For some of these, taking advantage of CLIP’s higher input resolution substantially improves results. It may be possible to get similar benefits from Imagen by incorporating scores from its superresolution models, which we leave for future work to explore.

We found that the boost from learned weightings is small, improving accuracies by around 1% on average. This result shows that our simple heuristic weighting function generalizes well across datasets. We found using no weights (i.e. $w_t = 1$) hurts performance substantially (e.g., CIFAR100 accuracy drops to 45%), which is a bit surprising because many diffusion models, including Imagen, are trained with no weights in their VLBs.

Imagen	CLIP	ViT-22B	ResNet50 (supervised)
84.4	51.6	68.7	79 (top-5)

Table 2. Percent shape accuracy for zero-shot classification on the Stylized Imagenet dataset.

4.2. Robustness to Texture Cues

We next study Imagen’s robustness to presence of texture cues in images by evaluating its performance on the Stylized Imagenet dataset from Geirhos et al. (2019). The dataset consists of Imagenet images altered to have a shape-texture conflict. While (for example) changing an image of a cat so it has a texture similar to elephant skin doesn’t confuse humans, it could cause a model to classify the image as an elephant. Geirhos et al. (2019) showed that CNNs trained on Imagenet were strongly biased towards recognising textures rather than shapes, which is in stark contrast to human behavioural evidence.

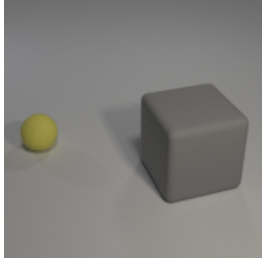
We test Imagen’s robustness to detecting shapes in presence of texture cues by using the same setting for classification as in Section 4.1. We report shape accuracy which is the percentage of images for which the model predicts the image’s shape correctly in Table 2. We compare Imagen with CLIP, the recently proposed ViT-22B model (Dehghani et al., 2023) which was trained on JFT (Sun et al., 2017) extended to 4B images (Zhai et al., 2022) and fine-tuned on Imagenet, and a (not zero-shot) supervised ResNet50 model trained on the training set. Imagen outperforms CLIP and ViT-22B model by more than 30% and 15% respectively, and the top-5 accuracy performance of the ResNet50 model by 5%.

We believe that the denoising process of the diffusion model is critical in removing the texture bias commonly observed in supervised convolutional models, making it robust to presence of texture based cues. These findings are in line with Nie et al. (2022), who achieve state-of-the-art adversarial robustness through denoising adversarial examples with a diffusion model.

4.3. Calibration

It is desirable for classifiers, especially when used in the zero-shot setting with possibly out-of-domain examples, to be well calibrated. In other words, if a classifier predicts a label \tilde{y}_i with probability p , the true label should be \tilde{y}_i roughly $100 \cdot p\%$ of the time. However, the diffusion model classifier does not directly produce probabilities for classes. While $p(y_i = y_k | \mathbf{x}_i)$ should roughly be proportional to the expectation in Equation (3) when exponentiated (i.e. we can apply a softmax to the average weighted scores to get probabilities), in practice our estimates of the expectations are very noisy and do not provide well-calibrated scores.

We propose a simple alternative that takes advantage of early pruning: we use the total number of diffusion model calls used for the image as a calibration measure. The intuition is that a harder example will require more scores to determine the arg min class with good statistical significance. We show reliability diagrams (DeGroot & Fienberg, 1983) and report Expected Calibration Error (Guo et al., 2017)



Attribute recognition tasks test if the model can identify basic image features by scoring an attribute in the image against one not present. Some example tasks/prompts are shown below:
 Shape: A **sphere**. vs. A **cylinder**. Color: A **gray object**. vs. A **red object**.

Binding tasks test if the model binds a given attribute to the correct object. For example:
 Color|Shape: A **yellow sphere**. vs. A **gray sphere**.
 Color|Position: On the right is a **gray object** vs. On the right is a **yellow object**.

Pair binding tasks are easier binding tasks where information about both objects is provided. For example:
 Shape,Size: A **small sphere and a large cube**. vs. A **large sphere and a small cube**.
 Color,Size: A **small yellow object and a large gray object**. vs. A **large yellow object and a small gray object**.

Figure 3. Examples of the synthetic-data attribute binding tasks. We explored more sophisticated prompts than in the figure (e.g., “A blender rendering of two objects, one of which is a yellow sphere.”), but they didn’t substantially change results.

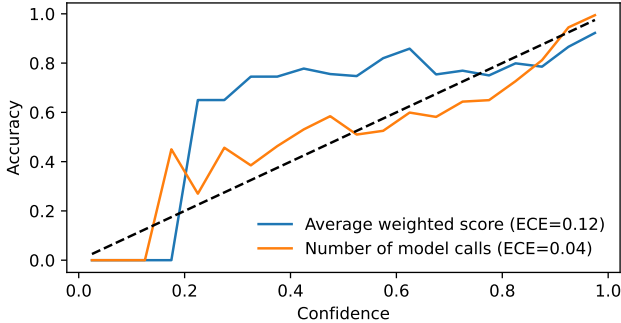


Figure 4. Model reliability diagram comparing confidence measures of Imagen on CIFAR-100. The number of model calls used in Algorithm 1 produces better-calibrated confidences than using the actual scores for different classes.

(ECE) for the methods in Figure 4. Using a small held-out set of examples, we apply temperature scaling (Guo et al., 2017) for the score-based confidences and Platt scaling (Platt et al., 1999) for the number-of-scores confidences, (see Appendix C for details). Number of scores is fairly well-calibrated, showing it is possible to obtain reasonable confidences from diffusion model classifiers despite them not providing a probability distribution over classes.

4.4. Evaluating Attribute Binding on Synthetic Data

We have shown that Imagen performs comparably to CLIP at few-shot classification, and much better than CLIP at disregarding misleading textural cue. Does Imagen have additional capabilities that are difficult to obtain through contrastive pre-training? We hypothesize that one such area may be in compositional generalization, and specifically compare Imagen and CLIP at attribute binding. Text-to-image generative models have shown emergent compositional generalization at large enough scale, being able to combine different concepts to handle prompts such as “a chair shaped like an avocado” (Ramesh et al., 2021). Attribute binding is a key piece of compositional reasoning, as it enables the understanding and integration of multiple concepts into a coherent whole. For example in the statement

“a yellow sphere and a gray cube” we understand the sphere is yellow and the cube is gray, not the other way around.

We test attribute binding in Imagen and CLIP on synthetic data. While previous work has examined attribute binding in text-to-image models by examining model generations (Nichol et al., 2021; Yu et al., 2022; Feng et al., 2023), our Imagen classifier offers a way of more precisely studying the question quantitatively. We hope in the future, this sort of study will be useful for comparing the abilities of generative image models at a fine-grained level.

Dataset Construction: We use the setup of Lewis et al. (2022), where images are generated based on the CLEVR (Johnson et al., 2017) visual question answering dataset. CLEVR images contain various object (cubes, cylinders, and spheres) with various attributes (different sizes, colors, and materials). A modified version of the CLEVR rendering script is used to generates images containing two objects of different shapes. From these images, we construct binary classification tasks of 1000 examples each; see Figure 3 for more details and examples. We follow the same setup as in the classification evaluation, using the 64x64 Imagen model with heuristic timestep weighting and largest public CLIP model (with full-resolution inputs).

Results: Scores for Imagen and CLIP at these tasks is shown in Table 3. On attribute recognition tasks Imagen and CLIP are able to identify shapes and colors that occur in the image with fairly high accuracy. Imagen is slightly worse at shape identification; we find most of these are due to it mixing up “cylinder” and “cube” when the objects are small. Mistakes in color recognition generally occur when the distractor color is similar to the true color or to the color of the other object in the image (e.g. the distractor color is blue and there is a large cyan object in the image).

We find that while CLIP can recognize image attributes, it performs no better than random chance for the attribute binding tasks, showing it is unable to connect attributes to objects on this data. In contrast, Imagen can perform (at least to some extent) the pair binding tasks, and does bet-

ter than chance on the Shape|Color and Color|Shape tasks. Part of Imagen’s advantage might be in its text encoder, the pre-trained T5 (Raffel et al., 2020) model. Saharia et al. (2022b) find that instead using CLIP’s text encoder for Imagen decreased its performance on generations involving specific colors or spatial positions. Similarly, Ramesh et al. (2022) find that DALLE-2, which uses a CLIP text encoder, is worse at attribute binding than GLIDE, which uses representations from a jointly-trained transformer processing the text. However, a perhaps more significant advantage of Imagen over CLIP is its use of cross attention to allow interaction between textual and visual features. A visual model without completely independent text and image encoders such as LXMERT (Tan & Bansal, 2019) or CMA-Clip (Liu et al., 2021) might perform better, but of course these models come with the added compute cost of having to process all image-text pairs with the model instead of embedding text and images separately.

One mistake we observed frequently in Color|Shape is Imagen preferring the color of the larger object in the image; e.g. scoring “A gray sphere” over “A yellow sphere” in Figure 3. We hypothesize that it is helpful for denoising at high noise levels when the text conditioning provides the color for a large region of the image, even when the color is associated with the wrong shape. In the pair task, the full color information for both objects is always provided, which avoids this issue, and perhaps explains why accuracies at pair tasks are much higher.

Previous work has qualitatively found that large image generation models sometimes struggle with spatial positioning (Yu et al., 2022). We find this to be mostly true for Imagen, which generally performs worst at the position tasks. Our tasks with position attributes are similar to the analysis in Subramanian et al. (2022), who also found CLIP does not do better than chance. We also found CLIP appears to have systematic position bias; preferring the caption with “right” in it over “left” 85% of the time for Shape|Position.

5. Conclusion

We have proposed a method that enables diffusion models to be used as zero-shot classifiers and developed ways of greatly improving its efficiency to make it usable. Our experiments with Imagen demonstrate strong results on image classification. Furthermore, we show Imagen is remarkably robust to misleading textures, achieving state-of-the-art results on Stylized Imagenet. While existing analysis of diffusion models usually studies generated images qualitatively, our framework provides a way of quantitatively evaluating text-to-image generative models through evaluating them on controlled classification tasks. We showcase this through our study on attribute binding, where we find that Imagen is sometimes able to bind attributes while CLIP

Task	Imagen	CLIP
Shape	85	91
Color	96	94
Shape Color	66/73	52/53
Shape Size	48/51	51/50
Shape Position	51/52	48/51
Color Size	54/54	51/48
Color Position	49/49	50/49
Size Position	50/54	50/48
Shape,Color	100	54
Shape,Size	99	52
Shape,Position	74	50
Color,Size	86	48
Color,Position	72	49
Size,Position	69	51

Table 3. Percent accuracy for models on zero-shot synthetic-data tasks investigating attribute binding. Bold results are significant ($p < 0.01$) according to a two-sided binomial test. For non-pair binding tasks, we show both directions (e.g. Shape|Color and Color|Shape before/after the slash. CLIP is unable to bind attributes, while Imagen sometimes can.

does not appear to have this ability.

We hope our findings will inspire future work in using text-to-image diffusion models as foundation models for tasks other than generation. One direction is fine-tuning diffusion models on downstream tasks; given the strong zero-shot performance of Imagen, a natural next step is evaluating it after further supervised training. Indeed, Brempong et al. (2022) already explore a related idea, finding that denoising pre-training can improve models on semantic segmentation.

We note that our main comparison in this work against CLIP is not direct in that the model architectures, parameter counts, and training data are different. As models become larger, a key question is how do the scaling laws (Hestness et al., 2017; Kaplan et al., 2020) of contrastive vs generative pre-training compare, which we leave as a question for future work. We are also interested in applying our analysis to other diffusion models to show that our results are not specific to Imagen. Towards this end, we are currently working on applying our method to Stable Diffusion (Rombach et al., 2022). Additionally, we are also interested to apply our analysis to other generative models and study to what extent our results are a consequence of generative pre-training generally compared to diffusion pre-training.

Ultimately, our method does not produce a practical classifier, as it requires substantial compute when scoring many classes. Instead, we see the main value of this work is in revealing more about the abilities of large pre-trained diffusion models. Our results suggest that generative pre-training may be a useful alternative to contrastive pre-training for text-image self-supervised learning.

Acknowledgements

We thank Kevin Swersky, Mohammad Norouzi, and David Fleet for helpful discussions and feedback, Martha Lewis and Ellie Pavlick for answering our questions about their CLIP attribute binding experiments, and Robert Geirhos for answering our questions about Stylized Imagenet and ViT-22B.

References

Amir Bar, Yossi Gandelsman, Trevor Darrell, Amir Globerson, and Alexei A Efros. [Visual prompting via image inpainting](#). *Advances in neural information processing systems*, 2022.

Emmanuel Asiedu Brempong, Simon Kornblith, Ting Chen, Niki Parmar, Matthias Minderer, and Mohammad Norouzi. [Denoising Pretraining for Semantic Segmentation](#). In *Proceedings of the IEEE/CVF Conference on Computer Vision and Pattern Recognition*, pp. 4175–4186, 2022.

Tom Brown, Benjamin Mann, Nick Ryder, Melanie Subbiah, Jared D Kaplan, Prafulla Dhariwal, Arvind Neelakantan, Pranav Shyam, Girish Sastry, Amanda Askell, et al. [Language models are few-shot learners](#). *Advances in neural information processing systems*, 33:1877–1901, 2020.

Ryan Burgert, Kanchana Ranasinghe, Xiang Li, and Michael S Ryoo. [Peekaboo: Text to Image Diffusion Models are Zero-Shot Segmentors](#). *arXiv preprint arXiv:2211.13224*, 2022.

Morris H DeGroot and Stephen E Fienberg. [The comparison and evaluation of forecasters](#). *Journal of the Royal Statistical Society: Series D (The Statistician)*, 32(1-2): 12–22, 1983.

Mostafa Dehghani, Josip Djolonga, Basil Mustafa, Piotr Padlewski, Jonathan Heek, Justin Gilmer, Andreas Steiner, Mathilde Caron, Robert Geirhos, Ibrahim Alabdulmohsin, et al. [Scaling vision transformers to 22 billion parameters](#). *arXiv preprint arXiv:2302.05442*, 2023.

Jia Deng, Wei Dong, Richard Socher, Li-Jia Li, Kai Li, and Li Fei-Fei. [Imagenet: A large-scale hierarchical image database](#). In *2009 IEEE conference on computer vision and pattern recognition*, pp. 248–255. Ieee, 2009.

Alexey Dosovitskiy, Lucas Beyer, Alexander Kolesnikov, Dirk Weissenborn, Xiaohua Zhai, Thomas Unterthiner, Mostafa Dehghani, Matthias Minderer, Georg Heigold, Sylvain Gelly, Jakob Uszkoreit, and Neil Houlsby. [An Image is Worth 16x16 Words: Transformers for Image Recognition at Scale](#). In *International Conference on Learning Representations*, 2021.

Weixi Feng, Xuehai He, Tsu-Jui Fu, Varun Jampani, Arjun Reddy Akula, P. Narayana, Sugato Basu, Xin Eric Wang, and William Yang Wang. [Training-Free Structured Diffusion Guidance for Compositional Text-to-Image Synthesis](#). In *International Conference on Learning Representations*, 2023.

Robert Geirhos, Patricia Rubisch, Claudio Michaelis, Matthias Bethge, Felix A Wichmann, and Wieland Brendel. [ImageNet-trained CNNs are biased towards texture; increasing shape bias improves accuracy and robustness](#). *International Conference on Learning Representations*, 2019.

Chuan Guo, Geoff Pleiss, Yu Sun, and Kilian Q Weinberger. [On calibration of modern neural networks](#). In *International conference on Machine Learning*, pp. 1321–1330. PMLR, 2017.

Kaiming He, Xinlei Chen, Saining Xie, Yanghao Li, Piotr Dollár, and Ross Girshick. [Masked autoencoders are scalable vision learners](#). In *Proceedings of the IEEE/CVF Conference on Computer Vision and Pattern Recognition*, pp. 16000–16009, 2022.

Joel Hestness, Sharan Narang, Newsha Ardalani, Gregory Diamos, Heewoo Jun, Hassan Kianinejad, Md Patwary, Mostafa Ali, Yang Yang, and Yanqi Zhou. [Deep learning scaling is predictable, empirically](#). *arXiv preprint arXiv:1712.00409*, 2017.

Jonathan Ho, Ajay Jain, and Pieter Abbeel. [Denoising diffusion probabilistic models](#). *Advances in Neural Information Processing Systems*, 33:6840–6851, 2020.

Chao Jia, Yinfei Yang, Ye Xia, Yi-Ting Chen, Zarana Parekh, Hieu Pham, Quoc Le, Yun-Hsuan Sung, Zhen Li, and Tom Duerig. [Scaling up visual and vision-language representation learning with noisy text supervision](#). In *International Conference on Machine Learning*, pp. 4904–4916. PMLR, 2021.

Justin Johnson, Bharath Hariharan, Laurens Van Der Maaten, Li Fei-Fei, C Lawrence Zitnick, and Ross Girshick. [CLEVR: A diagnostic dataset for compositional language and elementary visual reasoning](#). In *Proceedings of the IEEE conference on computer vision and pattern recognition*, pp. 2901–2910, 2017.

Jared Kaplan, Sam McCandlish, Tom Henighan, Tom B Brown, Benjamin Chess, Rewon Child, Scott Gray, Alec Radford, Jeffrey Wu, and Dario Amodei. [Scaling laws for neural language models](#). *arXiv preprint arXiv:2001.08361*, 2020.

Diederik Kingma, Tim Salimans, Ben Poole, and Jonathan Ho. [Variational diffusion models](#). *Advances in neural information processing systems*, 34:21696–21707, 2021.

Diederik P Kingma and Ruiqi Gao. [Understanding the Diffusion Objective as a Weighted Integral of ELBOs](#). *arXiv preprint arXiv:2303.00848*, 2023.

Diederik P Kingma and Max Welling. [Auto-encoding Variational Bayes](#). *International Conference on Learning Representations*, 2014.

Martha Lewis, Qinan Yu, Jack Merullo, and Ellie Pavlick. [Does CLIP Bind Concepts? Probing Compositionalty in Large Image Models](#). *arXiv preprint arXiv:2212.10537*, 2022.

Huidong Liu, Shaoyuan Xu, Jinmiao Fu, Yang Liu, Ning Xie, Chien-Chih Wang, Bryan Wang, and Yi Sun. [CMA-CLIP: Cross-modality attention clip for image-text classification](#). *arXiv preprint arXiv:2112.03562*, 2021.

Andrew Ng and Michael Jordan. [On discriminative vs. generative classifiers: A comparison of logistic regression and naive bayes](#). *Advances in neural information processing systems*, 14, 2001.

Alex Nichol, Prafulla Dhariwal, Aditya Ramesh, Pranav Shyam, Pamela Mishkin, Bob McGrew, Ilya Sutskever, and Mark Chen. [GLIDE: Towards Photorealistic Image Generation and Editing with Text-Guided Diffusion Models](#). In *International Conference on Machine Learning*, 2021.

Weili Nie, Brandon Guo, Yujia Huang, Chaowei Xiao, Arash Vahdat, and Anima Anandkumar. [Diffusion Models for Adversarial Purification](#). *International Conference on Machine Learning*, 2022.

OpenAI. [Prompt Engineering for Imagenet](#). *Github*, 2021a.

OpenAI. [Prompts for Datasets](#). *Github*, 2021b.

John Platt et al. [Probabilistic outputs for support vector machines and comparisons to regularized likelihood methods](#). *Advances in large margin classifiers*, 10(3):61–74, 1999.

Alec Radford, Jong Wook Kim, Chris Hallacy, Aditya Ramesh, Gabriel Goh, Sandhini Agarwal, Girish Sastry, Amanda Askell, Pamela Mishkin, Jack Clark, et al. [Learning transferable visual models from natural language supervision](#). In *International Conference on Machine Learning*, pp. 8748–8763. PMLR, 2021.

Colin Raffel, Noam Shazeer, Adam Roberts, Katherine Lee, Sharan Narang, Michael Matena, Yanqi Zhou, Wei Li, and Peter J Liu. [Exploring the limits of transfer learning with a unified text-to-text transformer](#). *The Journal of Machine Learning Research*, 21(1):5485–5551, 2020.

Aditya Ramesh, Mikhail Pavlov, Gabriel Goh, Scott Gray, Chelsea Voss, Alec Radford, Mark Chen, and Ilya Sutskever. [Zero-shot text-to-image generation](#). In *International Conference on Machine Learning*, pp. 8821–8831. PMLR, 2021.

Aditya Ramesh, Prafulla Dhariwal, Alex Nichol, Casey Chu, and Mark Chen. [Hierarchical text-conditional image generation with clip latents](#). *arXiv preprint arXiv:2204.06125*, 2022.

Robin Rombach, Andreas Blattmann, Dominik Lorenz, Patrick Esser, and Björn Ommer. [High-resolution image synthesis with latent diffusion models](#). In *Proceedings of the IEEE/CVF Conference on Computer Vision and Pattern Recognition*, pp. 10684–10695, 2022.

Chitwan Saharia, William Chan, Huiwen Chang, Chris Lee, Jonathan Ho, Tim Salimans, David Fleet, and Mohammad Norouzi. [Palette: Image-to-image diffusion models](#). In *ACM SIGGRAPH 2022 Conference Proceedings*, pp. 1–10, 2022a.

Chitwan Saharia, William Chan, Saurabh Saxena, Lala Li, Jay Whang, Emily Denton, Seyed Kamyar Seyed Ghasemipour, Burcu Karagol Ayan, S Sara Mahdavi, Rapha Gontijo Lopes, et al. [Photorealistic Text-to-Image Diffusion Models with Deep Language Understanding](#). *Advances in Neural Information Processing Systems*, 2022b.

Christoph Schuhmann, Richard Vencu, Romain Beaumont, Robert Kaczmarczyk, Clayton Mullis, Aarush Katta, Theo Coombes, Jenia Jitsev, and Aran Komatsuzaki. [Laion-400m: Open dataset of clip-filtered 400 million image-text pairs](#). *arXiv preprint arXiv:2111.02114*, 2021.

Jascha Sohl-Dickstein, Eric Weiss, Niru Maheswaranathan, and Surya Ganguli. [Deep unsupervised learning using nonequilibrium thermodynamics](#). In *International Conference on Machine Learning*, pp. 2256–2265. PMLR, 2015.

Yang Song and Stefano Ermon. [Improved techniques for training score-based generative models](#). *Advances in neural information processing systems*, 33:12438–12448, 2020.

Yang Song, Jascha Sohl-Dickstein, Diederik P Kingma, Abhishek Kumar, Stefano Ermon, and Ben Poole. [Score-based generative modeling through stochastic differential equations](#). *arXiv preprint arXiv:2011.13456*, 2020.

Sanjay Subramanian, Will Merrill, Trevor Darrell, Matt Gardner, Sameer Singh, and Anna Rohrbach. [ReCLIP: A Strong Zero-Shot Baseline for Referring Expression Comprehension](#). In *ACL*, 2022.

Chen Sun, Abhinav Shrivastava, Saurabh Singh, and Abhinav Gupta. Revisiting unreasonable effectiveness of data in deep learning era. In *Proceedings of the IEEE international conference on computer vision*, pp. 843–852, 2017.

Hao Tan and Mohit Bansal. **Lxmert: Learning cross-modality encoder representations from transformers**. *arXiv preprint arXiv:1908.07490*, 2019.

Pascal Vincent, Hugo Larochelle, Isabelle Lajoie, Yoshua Bengio, Pierre-Antoine Manzagol, and Léon Bottou. **Stacked denoising autoencoders: Learning useful representations in a deep network with a local denoising criterion**. *Journal of machine learning research*, 11(12), 2010.

Jiahui Yu, Yuanzhong Xu, Jing Yu Koh, Thang Luong, Gunjan Baid, Zirui Wang, Vijay Vasudevan, Alexander Ku, Yinfeng Yang, Burcu Karagol Ayan, et al. **Scaling autoregressive models for content-rich text-to-image generation**. *arXiv preprint arXiv:2206.10789*, 2022.

Lu Yuan, Dongdong Chen, Yi-Ling Chen, Noel Codella, Xiyang Dai, Jianfeng Gao, Houdong Hu, Xuedong Huang, Boxin Li, Chunyuan Li, et al. **Florence: A new foundation model for computer vision**. *arXiv preprint arXiv:2111.11432*, 2021.

Xiaohua Zhai, Alexander Kolesnikov, Neil Houlsby, and Lucas Beyer. **Scaling vision transformers**. In *Proceedings of the IEEE/CVF Conference on Computer Vision and Pattern Recognition*, pp. 12104–12113, 2022.

A. Learned Weighting Functions.

While for most experiments we use a heuristic weighting function for w_t , we also explored learning an effective weighting function (although this is not truly zero-shot). To do this, we aggregate scores for each image \mathbf{x} and class y_k into 20 buckets, with each bucket covering a small slice of timestep values:

$$b_i(\mathbf{x}, y_k) = \mathbb{E}_{\epsilon, t \sim \mathcal{U}[0.05i, 0.05(i+1)]} \|\mathbf{x} - \tilde{\mathbf{x}}_{\theta}(\mathbf{x}_t, \phi(y_k), t)\|_2^2$$

where we estimate the expectation with Monte Carlo sampling (typically around 100 samples). We then learn a 20-feature linear model with parameters $[\mathbf{v}_0, \dots, \mathbf{v}_{19}]$ over these buckets:

$$p_{\mathbf{v}}(y = y_k | \mathbf{x}) = \frac{\exp(\sum_{i=0}^{19} -\mathbf{v}_i \mathbf{b}_i(\mathbf{x}, y_k))}{\sum_{y_j \in [y_K]} \exp(\sum_{i=0}^{19} -\mathbf{v}_i \mathbf{b}_i(\mathbf{x}, y_j))}$$

trained with standard maximum likelihood over the data. At test-time we use the weighting

$$\mathbf{w}_t = \mathbf{v}_{\lfloor t/0.05 \rfloor}$$

We generally found that (1) learned weighting functions are pretty similar across datasets, and (2) the weighting functions are transferable: the \mathbf{v} s learned on one dataset get good accuracy when evaluated on other ones. On average, learned weights produced around 1% higher accuracy on zero-shot classification tasks, but we omitted the results from the main paper because using learned weights is not truly zero-shot.

B. Variances in Classification Accuracies.

Due to our reduced-size evaluation sets, variances in accuracy on zero-shot classification tasks across different random splits are roughly $\pm 0.4\%$ for CLIP and $\pm 0.7\%$ for Imagen. Imagen has higher variance due to the inherent randomness in noising images (while CLIP is deterministic). Overall, we are not interested in small accuracy differences anyway, as the comparison between Imagen and CLIP is non-direct in various ways; instead we are trying to get a broad understanding of Imagen’s abilities.

C. Calibration Details

We considered two methods for calibrating Imagen’s scores in Section 4.3; here we briefly go into more mathematical detail on how they work.

Temperature-scaled raw scores. We use $s_{y_k}(\mathbf{x})$ to denote the weighted average squared error for class y_k on image \mathbf{x} , i.e., the Monte-Carlo estimate for the re-weighted VLB in equation 3. We turn these scores into an estimated

probability by applying a softmax with temperature:

$$p_\theta(y = y_k | \mathbf{x}) = \frac{\exp(-s_{y_k}(\mathbf{x})/\tau)}{\sum_{y_j \in [y_K]} \exp(-s_{y_j}(\mathbf{x})/\tau)}$$

Note that this approach requires good score estimates for each class, so it is not compatible with the class pruning method presented in Section 3.1.

Platt-scaled number of scores. Our other confidence method relies on the total number of scores needed to eliminate all other classes as candidates. Let $\tilde{y}(\mathbf{x})$ denote the predicted class for example \mathbf{x} and $n(\mathbf{x})$ be the total number of calls to \tilde{x}_θ used to obtain the prediction when running Algorithm 1. Then we estimate

$$p_\theta(y = \tilde{y}(\mathbf{x}) | \mathbf{x}) = \text{sigmoid}(-n(\mathbf{x})/\tau + \beta)$$

We learn τ (and β for Platt scaling) on a small held-out set of examples.

D. Details on Attribute Binding Tasks and Prompts

We use the relational dataset from Lewis et al. (2022) for the attribute binding experiments. Each image consists of two objects of different shapes and colors; for tasks involving size we filter out examples where both objects are the same size. Each image contains two objects with different attributes $\text{shape} \in \{\text{cube}, \text{sphere}, \text{cylinder}\}$, $\text{color} \in \{\text{blue}, \text{cyan}, \text{blue}, \text{brown}, \text{gray}, \text{green}, \text{purple}, \text{red}, \text{yellow}\}$, $\text{size} \in \{\text{small}, \text{large}\}$, and $\text{position} \in \{\text{left}, \text{right}\}$.

Given a task (e.g. Shape|Size), we construct a task-specific description for an object as follows:

“On the {position} is a ” if Position tasks else “A ”+
“size ” if Size task else “”+
“color ” if Color task else “”+
“shape.” if Shape task else “object.”

For recognition and binding tasks, we randomly select one of the two objects in the image to be the positive example and then use its description as the positive prompt. For pair tasks, we join the descriptions for both objects together with “and” (removing the period from the first description and lowercasing the second one) for the positive prompt.

To construct a negative example for recognition tasks, we replace the positive attribute with a random attribute not in the image. For binding tasks, we replace one of positive description’s attributes with the other object’s attribute (e.g., for Shape|Color, we replace shape).

For pair tasks, there is a choice in how the two objects are ordered (e.g. “On the left is a cube and on the right is a

sphere” vs “On the right is a sphere and on the left is a cube”. We follow the preference of stating the leftmost position/shape/color/size first in that order. For example, this means we will always start with “On the left...” rather than “On the right...”. Similarly, the negative example for Color,Size in Figure 3 is “A large yellow object and small gray object” rather than “A small gray object and a large yellow object” because we prefer to first put the leftmost color over the leftmost size.

We experimented with a variety of other prompts, but found none to work substantially better than these simple ones.